Available online at www.sciencedirect.com
ScienceDirect
Trans. Nonferrous Met. Soc. China 25(2015) 3886−3892
Transactions of Nonferrous Metals Society of China
www.tnmsc.cn

Effect of individual and combined additions of Al−5Ti−B, Mn and Sn on sliding wear behavior of A356 alloy

Ke QIU[1], Ri-chu WANG[1], Chao-qun PENG[1], Nai-guang WANG[2], Zhi-yong CAI[1], Chun ZHANG[1]

1. School of Materials Science and Engineering, Central South University, Changsha 410083, China;
2. School of Metallurgy and Environment, Central South University, Changsha 410083, China

Received 10 August 2015; accepted 25 October 2015

Abstract: The effect of grain refiner, Mn and Sn additions on the sliding wear behavior of A356 aluminum alloys was investigated. The microstructure and worn surfaces of the studied alloys were characterized by optical microscopy (OM), scanning electron microscopy (SEM), and transmission electron microscopy (TEM). The experimental results indicate that the alloy refined by Al−5Ti−B alloy exhibits equiaxed α(Al) dendrites and performs better wear resistance compared with the alloy without the grain refiner. Moreover, the addition of Mn can change the β-Al_5FeSi phase to α-Al(Mn,Fe)Si phase and reduce the possibility of crack formation, thus improving the wear resistance. Sn added to A356 aluminum alloy forms Mg_2Sn precipitates after heat treatment. Therefore, the unrealizable precipitation hardening Mg_2Si phase and the softening β-Sn phase can reduce the hardness of the alloy, and finally reduce the wear resistance.

Key words: A356 aluminum alloy; dry sliding; wear; grain refinement; manganese; tin

1 Introduction

It is well-known that cast Al−Si alloys has been widely used in automobile, marine, and aircraft industries due to the excellent fluidity, corrosion resistance, and mechanical properties [1,2]. However, the common impurity, i.e., iron, in Al−Si alloys is detrimental to the mechanical properties. The formation of iron intermetallic compound, β-Al_5FeSi, which appears as needles or plate-like morphology, suffers the severe stress concentration due to its sharp edges [3]. This behavior would lead to the brittleness and hence has negative effect on the mechanical properties of the alloy. Attempts have been made to neutralize the harmful influences of iron intermetallics with the additions of Mn, Be, Cr, and Ca [4,5]. Among these elements, Mn is the most commonly used one due to the economic consideration. Alloying with appropriate amount of Mn, the β-Al_5FeSi needles can convert to less harmful intermetallic compound, i.e., α-$Al_{15}(Fe,Mn)_3Si_2$ Chinese scripts phase.

Compared with Mn, which is widely used for modification of Fe-intermetallics, Sn is not a common element in Al−Si cast alloys due to its mutual solid insolubility in Al. However, it has been reported that there are some advantages for adding Sn to Al−Si alloys. According to KLIAUGA et al [6], Sn has a "cleaning effect" on A356 aluminum alloys, which can remove iron and other impurities from solid solution and reduce the volume fraction of iron-rich intermetallics. They also found that adding 0.5% Sn in Al−7Si−Mg alloys can improve flow behavior, increase mould-filling capabilities, and reduce liquid segregation [7]. MOHAMED et al [8] has reported that better mechanical properties were shown with the addition of 0.05% Sn in A356.2 aluminum alloy.

Wear resistances of Al−Si alloys are influenced by many factors such as hardness, strength, ductility, shape, and size of microstructure constituents. Apart from these, wear resistances of Al−Si alloys are also affected by the practical conditions like pressure, speed, temperature, and rubbing surface [9]. The physical and mechanical properties of these alloys are greatly influenced by chemical composition. A great deal of researches have been done to study the effect of chemical composition on the wear behavior of Al−Si alloys [10−14]. However, there has been less work devoted to investigating the effect of combined additions of Mn and Sn on the wear characteristics of Al−Si alloys. In this work, an attempt

Corresponding author: Ri-chu WANG; Tel: +86-731-88836638; E-mail: rcwcsu@163.com
DOI: 10.1016/S1003-6326(15)64081-X

has been made to study the role of intermetallic compounds on the dry sliding wear behavior of Al−Si alloys with the additions of Mn and Sn. The influences of combined additions of Sr modifier and Al−5Ti−B grain refiners on the wear behavior of the alloys were also studied.

2 Experimental

Binary Al−22Si master alloy was made in an induction furnace by mixing commercial purity aluminum and silicon. Ternary Al−7Si−0.35Mg alloy was prepared from commercial purity aluminum, magnesium, and Al−22Si master alloy in 4 kg capacity SiC crucibles in an electric resistance furnace, which was held at (750±5) °C. The melt was covered by the cover agent containing NaCl, KCl, and NaF. Al−10Sr master alloy was added to ensure that the Sr level in the melt reached about 0.03%. Al−5Ti−B master alloy was chosen as the grain refiner and its amount was 1% for each alloy to ensure that no poisoning effect could happen. To study the combined effect of Mn and Sn on sliding, Al−15Mn master alloy and commercial pure tin were added to obtain the desired levels. The melt was thoroughly stirred with pure carbon rod and degassed with hexachlorothane. The holding time was over 15 min for enough incubation of Sr modification. The molten metal was poured into an L-shaped rectangular ZnO-coated metallic mold preheated at 250 °C. The as-cast alloy was subjected to T6 heat treatment, i.e., 8 h solution at 540 °C followed by water quenching, and 6 h aging at 160 °C.

The chemical compositions of various alloys determined by optical emission spectroscopy are shown in Table 1. Microstructure characterization was carried out by optical microscopy (OM) on the samples etched with an aqueous solution of 0.5% HF. Scanning electron microscopy (SEM) and transmission electron microscopy (TEM) were also adopted for further microstructure examination. TEM thin foils were prepared by the mechanical pitting and ion beam thinning at 5 kV.

Table 1 Chemical compositions of various aluminum alloys (mass fraction, %)

Alloy code	Si	Mg	Fe	Mn	Sn	Sr	Al
A356un[a]	6.95	0.33	0.52	0.001	0.001	0.03	Bal.
A356	6.96	0.32	0.51	0.001	0.001	0.03	Bal.
A356Mn1	7.03	0.30	0.51	0.13	0.001	0.03	Bal.
A356Mn2	6.92	0.34	0.53	0.32	0.001	0.03	Bal.
A356Mn3	7.08	0.32	0.50	0.49	0.001	0.03	Bal.
A356Sn1	6.95	0.33	0.51	0.006	0.12	0.03	Bal.
A356Sn2	7.02	0.32	0.55	0.002	0.29	0.03	Bal.
A356Sn3	7.08	0.33	0.50	0.002	0.58	0.03	Bal.
A356MnSn	6.98	0.33	0.50	0.51	0.47	0.03	Bal.

[a] un-grain refined

Hardness test plates (2.5 cm × 2.0 cm × 2.0 cm) were cut from the as-cast alloys. The surfaces were polished with fine sandpaper to remove any machining marks. The hardness measurements were carried out on the T6-treated samples using a Brinell hardness tester, employing a steel ball with 5 mm in diameter, and a load of 2.452 kN applied for 30 s. The average of five readings per test plate was taken to represent its hardness value.

Reciprocating dry wear testing was performed using UMT−3 at room temperature. A *d*9.5 mm Al_2O_3 ball was used as a counterpart. The top surface of the samples was ground using fine grit SiC paper and all the samples were ultrasonically cleaned in alcohol bath for 5 min before testing. The tests were performed in the condition of normal loads of 5, 15, 25, 35 N. The worn surfaces of wear test specimens were characterized by SEM microanalysis.

3 Results and discussion

3.1 Microstructure

The optical microstructure images of the as-cast A356 aluminum alloy with and without the addition of grain refiner are shown in Figs. 1(a) and (b), respectively. Both alloys are well modified because the coarse acicular eutectic Si alters to fibrous shape. In the absence of grain refiner, the A356 aluminum alloy exhibits a columnar α-dendritic structure shown in Fig. 1(a). However, with the addition of Al−5Ti−B master alloy, Fig. 1(b) reveals that the A356 aluminum alloy shows a partial response towards grain refinement with structural transition from columnar dendrites to equiaxed dendrites. This is due to the fact that a thin $TiAl_3$ layer has an affinity to segregate onto the surface of TiB_2 and these duplex particles act as the nucleation sites [15].

Figure 2 shows the SEM images of the intermetallic compounds in A356 aluminum alloys with different additions of alloying elements after T6 heat treatment. It can be seen from Figs. 2(a) and (b) that Mn makes the needle-type β-Al_5FeSi convert to α-Al(Mn,Fe)Si with Chinese script morphology. The rod-like α-Al(Mn,Fe)Si with branched distribution morphology is also observed, as consistent with SHABESTARI et al [16]. With the addition of tin, precipitation of β-Sn inside the eutectic region can be clearly seen in Fig. 2(c). Sn has low solubility both in Al and Si, and therefore β-Sn preferentially locates at the Al−Si interface and inside the eutectic Si regions at the end of solidification. The intermetallic compounds of the combined addition of Mn and Sn are shown in Fig. 2(d). While most β-Sn phases are distributed inside the eutectic Si regions, Chinese

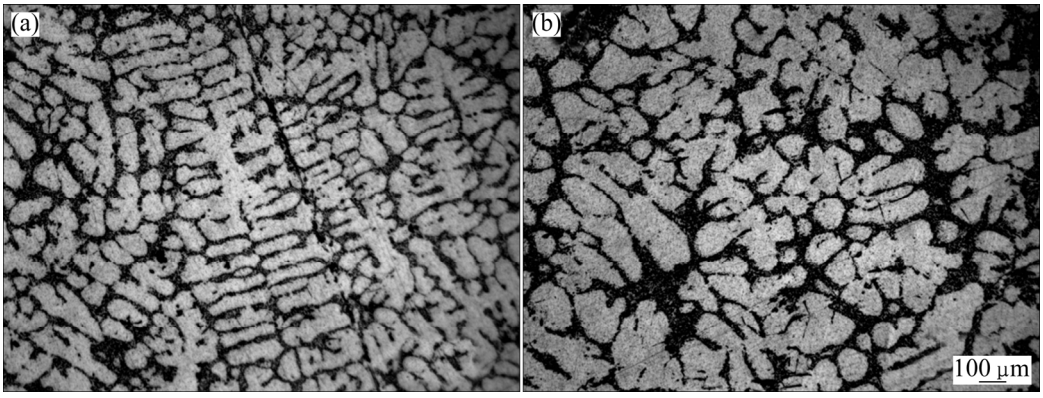

Fig. 1 Optical micrographs of as-cast A356 alloy: (a) Without grain refiner; (b) With Al−5Ti−B grain refiner

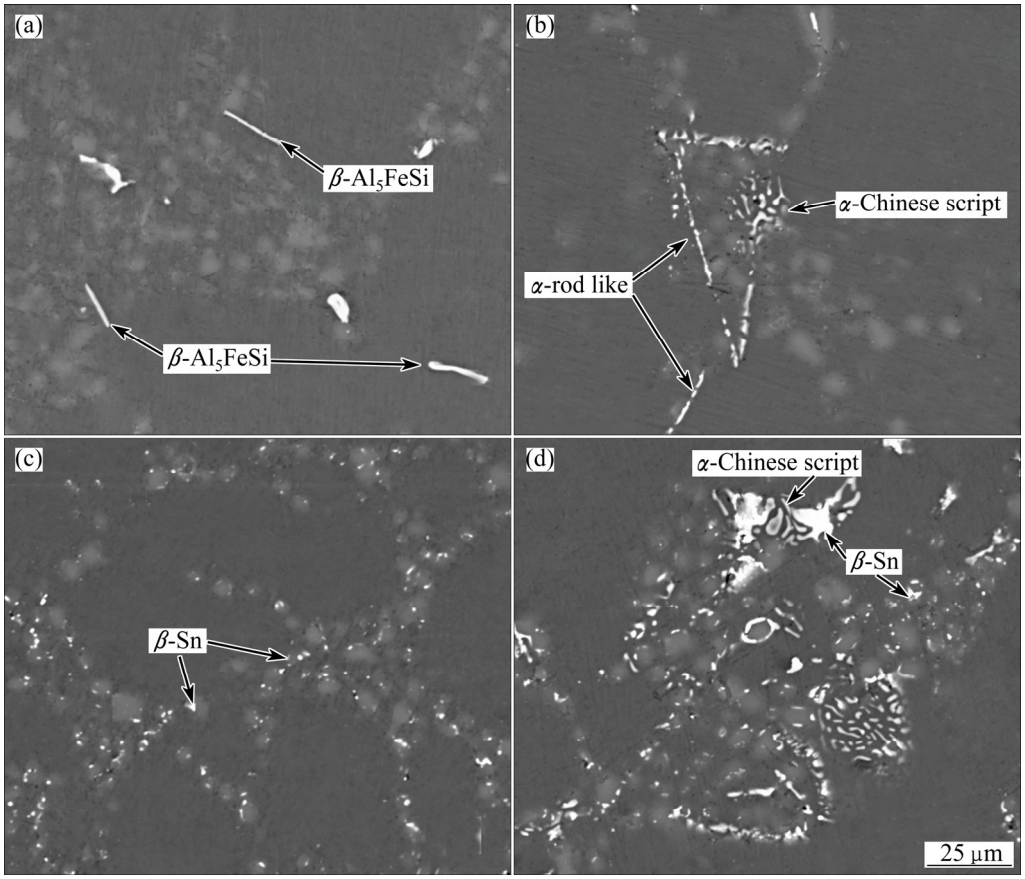

Fig. 2 SEM images of intermetallic compounds in different compositional alloys: (a) A356 alloy; (b) A356Mn3 alloy; (c) A356Sn1 alloy; (d) A356MnSn alloy

script α-Al(Mn,Fe)Si intermetallics are detected across the matrix and eutectic regions. Mg has higher affinity with Si and Sn than Al, TEM observation of Mg-intermetallic compound of A356Sn1 alloy is shown in Fig. 3. The composition of these particles is identified by X-ray mapping, confirming that the intermetallics are Mg_2Sn precipitates. In this study, it seems that Sn tends to interact with Mg more easily than Si, as consistent with MOHAMED et al [8]. However, the morphology of Mg_2Sn in Ref. [8] performs as Chinese scripts, which is not the same in this work.

3.2 Wear behavior

Figure 4 represents the variation of mass loss and the coefficient of friction (COF) as a function of applied load for the alloys added with different amounts of Al−5Ti−B grain refiner and Mn under constant sliding speed and at constant sliding distance. It can be seen from Figs. 4(a) and (b) that both mass loss and COF increase with increasing applied load. The mass loss and COF are higher in the case of non-grain refinement conditions. The alloy added with Mn has lower mass loss and COF compared with the A356 base alloy at all

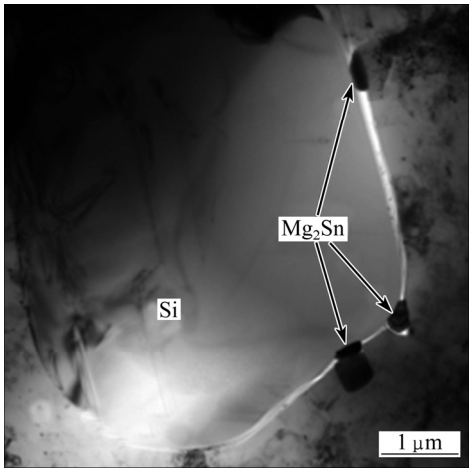

Fig. 3 TEM image showing Mg_2Sn precipitating at Al/Si interface

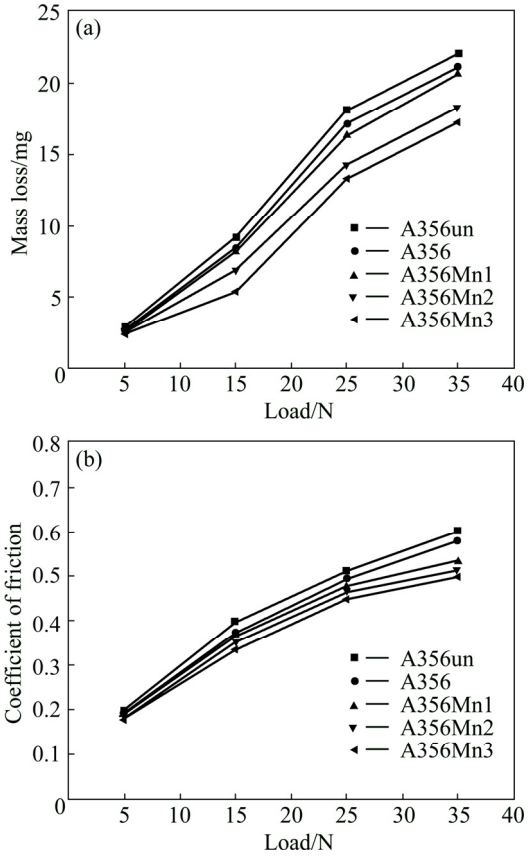

Fig. 4 Wear behavior of A356 alloys with grain refinement and Mn addition: (a) Variation of mass loss with different applied load; (b) Variation of coefficient of friction with different applied load

applied loads. It is noticeable that increasing Mn content can improve the wear resistance. Better wear resistance can be achieved via fine equiaxed primary α(Al) grains and uniform distribution of the second phase particles [17]. The structure of un-grain refined alloy exhibits coarse columnar α(Al) dendrites and does not have undesirable toughness and ductility. As shown in Table 2, the A356 aluminum alloy without grain refinement has lower hardness compared with the well grain refined alloy. The wear data support the microstructure as shown in Fig. 1. Needle-like β-Al_5FeSi phase is the common intermetallic compound in Al−Si alloys. Due to its hard and brittle characteristic, it exhibits low bond strength with the matrix and the sharp edges of β-needles introduce severe stress concentrations in the matrix of the alloy [3,11]. According to Fig. 4, the enhancement in the wear resistance of A356Mn3 added with Mn is originated from the modification of β-phase to Chinese script α-intermetallic compounds, as shown in Fig. 2(b). This modified morphology, compared with the needle-like β-phase, forms a rough interface with the matrix. The better bonding with matrix reduces the possibility of crack formation at the interface of intermetallic compounds with the matrix.

Table 2 Hardness of alloys with individual and combined addition of Mn and Sn after T6 heat treatment

Alloy code	Hardness (HB)
A356un	85.5
A356	93.3
A356Mn1	98.2
A356Mn2	101.2
A356Mn3	103.7
A356Sn1	70.1
A356Sn2	66.5
A356Sn3	66.7
A356MnSn	68.3

Figure 5 displays the effect of Sn content and combined additions of Mn and Sn on the A356 alloy with different applied loads. It is clear that both mass loss and COF of the alloys increase with increasing pressure in all the cases studied. The mass loss and COF are higher in the case of Sn addition. The hardness of the alloys in Fig. 5 is shown in Table 2. It is observed that the addition of 0.29% Sn to A356 alloy decreases the hardness from HB 93.3 to HB 66.5. Further addition of Sn does not decrease the hardness obviously. This observation may be ascribed to the formation of Mg_2Sn shown in Fig. 3. The presence of Mg_2Sn phase is not available for precipitation hardening during aging compared with Mg_2Si phase. Moreover, as shown in Fig. 2(c), β-Sn phase is formed inside the eutectic Si region. The soft β-Sn phase is also another reason for the reduction of hardness [8]. Therefore, the lower wear resistance of A356 aluminum alloy with Sn addition results from the reduction of hardness. It is reported that addition of Sn can improve wear resistance in hypereutectic Al−Si alloys [18]. However, the experimental results in this work show that the hardness seems to govern the wear

resistance of the alloys. Another reason for the reduction of wear resistance may be attributed to the Mg_2Sn−Sn eutectic formation [8], which can increase porosity in the alloys, thus increase the possibility of micro-crack formation.

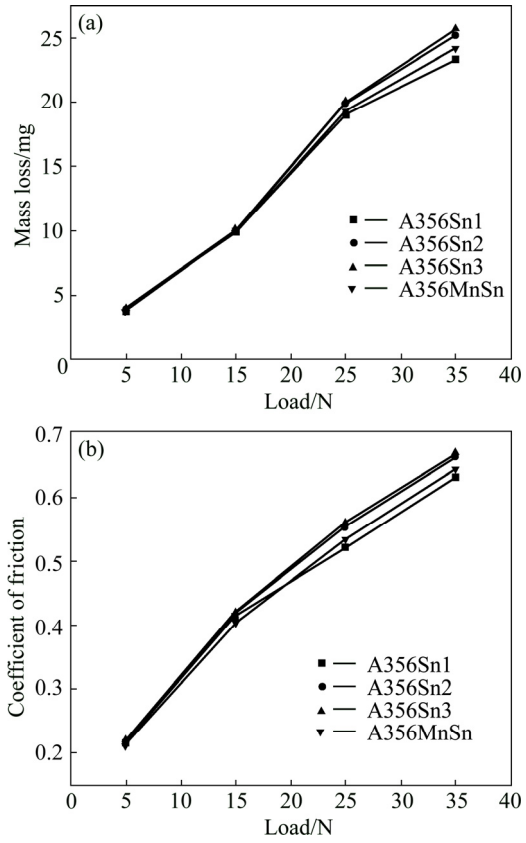

Fig. 5 Wear behavior of A356 alloys with individual addition of Sn and combined additions of Mn and Sn: (a) Variation of mass loss with different applied loads; (b) Variation of coefficient of friction with different applied loads

Figure 5 also shows the variation of mass loss and COF with different applied loads for combined additions of Mn and Sn. It can be seen that the A356 alloys doped with both Mn and Sn represent lower wear resistance compared with the A356 alloy shown in Fig. 4. Table 2 indicates that these alloys added with Mn and Sn also exhibit lower hardness. The hardness and wear properties can be explained based on the microstructure features of the alloys shown in Fig. 2(d). The addition of Mn can neutralize the harmful effect of β-Al_5FeSi phase. However, Sn addition leads the formation of soft β-Sn phase and precipitation of Mg_2Sn is not available for precipitation hardening during aging.

3.3 Worn surfaces

Worn surfaces of the A356 alloys listed in Table 1 were characterized by SEM. Figures 6(a) and (b) show the SEM images of worn surfaces of A356 alloys with and without the addition of Al−5Ti−B grain refiner, respectively. Each of the alloys was subjected to dry sliding wear test under the constant conditions of 25 N normal pressure, 604 r/min rotating speed. The worn surfaces in Fig. 6 display obvious craters and wear grooves. The craters on the worn surface are formed due to the removal of mechanically mixed layer. Both well modified alloys shown in Fig. 1 indicate that eutectic Si particles are fine. During sliding, the worn surface is covered with small and spherical silicon particles, which in turn protect the surface from wear and lead to less damage of the material. A comparison of Figs. 6(a) and (b) clearly reveals that the cracking of the surface and the formation of cavities happen during sliding test in the absence of grain refiner. Nevertheless, the surface possessing fewer cracks is observed with the addition of Al−5Ti−B master alloy as shown in Fig. 6(b). Crack nucleation generally occurs at some depth below the surface rather than near the surface. Thus, once a crack is nucleated, its propagation is slow owing to the presence of fine equiaxed primary α(Al) grains and particles. Moreover, it is suggested that grain refined alloys with finer dispersed particles undergo greater strain hardening [17]. Therefore, the comparison of worn surfaces supports better wear performance with the addition of Al−5Ti−B grain refiner as shown in Fig. 4.

Figure 7 shows the worn surfaces of different compositions of A356 alloys under constant conditions

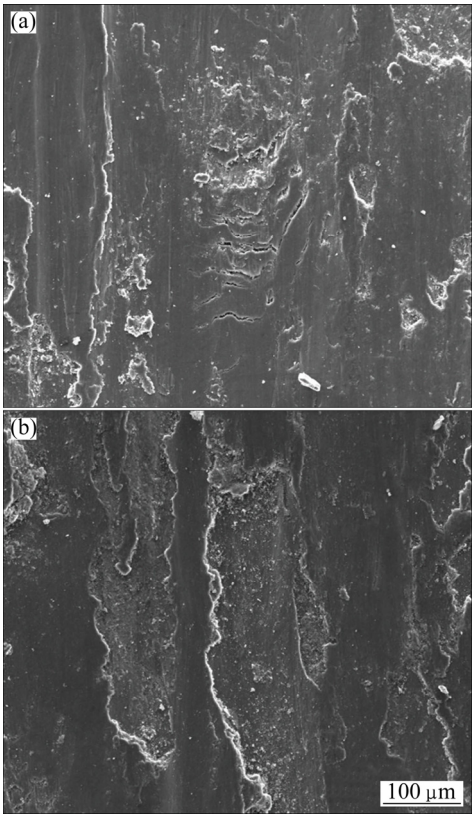

Fig. 6 SEM images of worn surfaces of A356 alloys: (a) Without grain refiner; (b) With Al−5Ti−B grain refiner

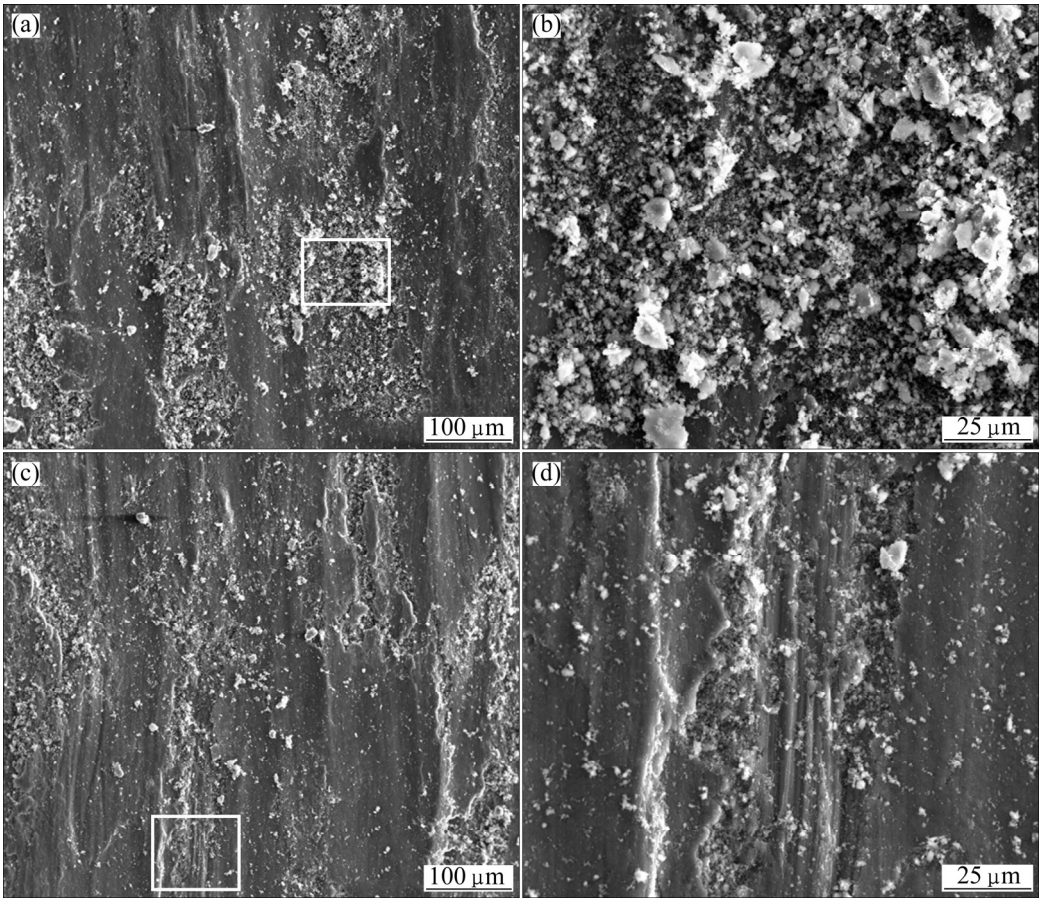

Fig. 7 SEM images of worn surfaces of A356 alloys: (a) A356Mn3 alloy; (b) High magnification image in (a); (c) A356MnSn alloy; (d) High magnification image in (c)

of applied load of 15 N and 604 r/min rotating speed.

Figure 7(a) shows the SEM image of A356 alloy with Mn addition (A356 Mn3) and Fig. 7(b) shows the higher magnification of the same alloy. The worn surface of A356 alloy with combined additions of Mn and Sn is shown in Figs. 7(c) and (d). Both alloys show plastic deformation and abrasion grooves, indicating the combination of adhesive wear and abrasion wear. It can also be observed that the worn surface of A356Mn3 alloy is mostly covered by some particles. Since the needle β-Al_5FeSi is modified to α-Al(Mn,Fe)Si, it has little effect on the formation of surface and subsurface micro-cracks. The particles on the surface are attributed to the entrapment of wear debris under the reciprocating sliding condition. Figure 7(d) reveals that A356MnSn alloy is subjected to more damage in terms of craters and groove than that of A356Mn3 alloy. This is probably due to the reduction of hardness of A356MnSn alloy surface as a result of Mg_2Sn precipitation. Since abrasion of a material is governed by its hardness [19], A356 alloy with Mg_2Sn precipitates is subjected to greater abrasion than that on the wear surface of an alloy with Mg_2Si precipitates due to the low hardness. This observation is also consistent with the wear test results.

4 Conclusions

1) The addition of Al−5Ti−B grain refiner to Sr-modified A356 alloy can change the α(Al) structure from columnar to equiaxed dendrites and enhance the wear resistance.

2) The addition of Mn can modify the needle-like β-Al_5FeSi phases to α-intermetallics, which causes improvement of the wear resistance of the alloy.

3) Alloying with Sn in A356 alloy can cause the formation of Mg_2Sn and β-Sn phases. The soft β-Sn phase and the absence of precipitation hardening Mg_2Si phase lead to a reduction of hardness of the alloy, which exhibits lower wear resistance.

References

[1] CHEN Rui, SHI Yu-feng, XU Qing-yan, LIU Bai-cheng. Effect of cooling rate on solidification parameters and microstructure of Al−7Si−0.3Mg− 0.15Fe alloy [J]. Transactions of Nonferrous Metals Society of China, 2014, 24(6): 1645−1652.

[2] SUN Shao-chun, YUAN Bo, LIU Man-ping. Effects of moulding sands and wall thickness on microstructure and mechanical properties of Sr-modified A356 aluminum casting alloy [J].

Transactions of Nonferrous Metals Society of China, 2012, 22(8): 1884−1890.
[3] SEIFEDDINE S, JOHANSSON S, SVENSSON I L. The influence of cooling rate and manganese content on the β-Al_5FeSi phase formation and mechanical properties of Al−Si-based alloys [J]. Materials Science and Engineering A, 2008, 490: 385−390.
[4] SREEJA KUMARI S S, PILLAI R M, RAJAN T P D, PAI B C. Effects of individual and combined additions of Be, Mn, Ca and Sr on the solidification behaviour, structure and mechanical properties of Al−7Si−0.3Mg−0.8Fe alloy [J]. Materials Science and Engineering A, 2007, 460−461: 561−573.
[5] CHEN Z W, HAO X L, ZHAO J, MA C Y. Kinetic nucleation of primary α(Al) dendrites in Al−7%Si−Mg cast alloys with Ce and Sr additions [J]. Transactions of Nonferrous Metals Society of China, 2013, 23(12): 3561−3567.
[6] KLIAUGA A M, VIEIRA E A, FERRANTE M. The influence of impurity level and tin addition on the ageing heat treatment of the 356 class alloy [J]. Materials Science and Engineering A, 2008, 480: 5−16.
[7] VIEIRA E A, KLIAUGA A M, FERRANTE M. Microstructural evolution and rheological behaviour of aluminium alloys A356, and A356 + 0.5% Sn designed for thixocasting [J]. Journal of Materials Processing Technology, 2004, 155−156: 1623−1628.
[8] MOHAMED A M A, SAMUEL F H, SAMUEL A M, DOTY H W, VALTIERRA S. Influence of tin addition on the microstructure and mechanical properties of Al−Si−Cu−Mg and Al−Si−Mg casting alloys [J]. Metallurgical and Materials Transactions A, 2008, 39: 490−501.
[9] SHABEL B S, GRANGER D A, TRUCKNER W G. Friction and wear of aluminum-silicon alloys [J]. ASM Handbook, 1992, 18: 785−794.
[10] KORI S A, PRABHUDEV M S. Sliding wear characteristics of Al−7Si−0.3Mg alloy with minor additions of copper at elevated temperature [J]. Wear, 2011, 271: 680−688.
[11] ABOUEI V, SHABESTARI S G, SAGHAFIAN H. Dry sliding wear behaviour of hypereutectic Al−Si piston alloys containing iron-rich intermetallics [J]. Materials Characterization, 2010, 61: 1089−1096.
[12] CHANDRASHEKHARAIAH T M, KORI S A. Effect of grain refinement and modification on the dry sliding wear behaviour of eutectic Al−Si alloys [J]. Tribology International, 2009, 42: 59−65.
[13] DWIVEDI D K. Wear behaviour of cast hypereutectic aluminium silicon alloys [J]. Materials & Design, 2006, 27: 610−616.
[14] YANG C Y, LEE S L, LEE C K, LIN J C. Effects of Sr and Sb modifiers on the sliding wear behavior of A357 alloy under varying pressure and speed conditions [J]. Wear, 2006, 261: 1348−1358.
[15] MOHANTY P S, GRUZLESKI J E. Grain refinement mechanisms of hypoeutectic Al−Si alloys [J]. Acta Materialia, 1996, 44: 3749−3760.
[16] SHABESTARI S, MAHMUDI T, EMAMY M, CAMPBELL T. Effect of Mn and Sr on intermetallics in Fe-rich eutectic Al−Si alloy [J]. International Journal of Cast Metals Research, 2002, 15: 17−24.
[17] BASAVAKUMAR K G, MUKUNDA P G, CHAKRABORTY M. Influence of grain refinement and modification on dry sliding wear behaviour of Al−7Si and Al−7Si−2.5Cu cast alloys [J]. Journal of Materials Processing Technology, 2007, 186: 236−245.
[18] WU X F, ZHANG G A. Effect of Sn addition on microstructure and dry sliding wear behaviors of hypereutectic aluminum–silicon alloy A390 [J]. Journal of Materials Science, 2011, 46: 7319−7327.
[19] REDDY T V S, DWIVEDI D K, JAIN N K. Adhesive wear of stir cast hypereutectic Al−Si−Mg alloy under reciprocating sliding conditions [J]. Wear, 2009, 266: 1−5.

单独或复合添加 Al−5Ti−B、Mn 和 Sn 对 A356 铝合金滑动磨损性能的影响

邱 科[1]，王日初[1]，彭超群[1]，王乃光[2]，蔡志勇[1]，张 纯[1]

1. 中南大学 材料科学与工程学院，长沙 410083；
2. 中南大学 冶金与环境学院，长沙 410083

摘 要：研究添加 Al−5Ti−B、Mn 和 Sn 对 A356 铝合金滑动磨损性能的影响。采用光学显微镜、扫描电镜和透射电镜观察合金的显微组织和磨损表面。结果表明，Al−5Ti−B 晶粒细化的合金具有 α(Al)等轴晶组织，比未细化合金具有更好的抗磨损性能。另外，Mn 元素的添加能使 β-Al_5FeSi 转变成 α-Al(Mn,Fe)Si 相，减少裂纹形成的倾向并提高合金的抗磨损性能。A356 合金中添加 Sn 会形成 Mg_2Sn 相，导致合金不能形成 Mg_2Si 析出强化相；同时软化的 β-Sn 相会降低合金的硬度并最终降低合金的抗磨损性能。

关键词：A356 铝合金；干摩擦；磨损；晶粒细化；锰；锡

(Edited by Yun-bin HE)